

EVALUATION OF IMAGING TECHNIQUE ACCURACY FOR DISCHARGE
MEASUREMENT AND DEVELOPMENT OF REAL TIME SYSTEM FOR SURFACE
FLOW MEASUREMENT

By

Ichiro Fujita

Department of Civil Engineering, Graduate School of Engineering, Kobe University, Nada, Kobe, Japan

Hiroki Hara

Graduate Student, Department of Civil Engineering, Graduate School of Engineering, Kobe University, Nada,
Kobe, Japan

and

Atsuhiko Yorozya

International Centre for Water Hazard and Risk Management under the auspices of UNESCO (ICHARM)
Public Works Research Institute, 1-6, Minamihara, Tsukuba 305-8515, Japan

SYNOPSIS

The monitoring of river flow is a matter of vital importance to the management of river flows as well as the utilization of rivers and their environments. As for the flow measurement by imaging techniques using a monitoring camera, skepticism has still remained about the fundamental of the method. Therefore, in order to confront such skepticism we conducted concurrent measurements of a river flow by using imaging techniques as well as ADCP at the upstream of Tone River. It was made clear that the water surface velocity distributions measured by imaging techniques agree fairly well with the velocity distribution at the water surface extrapolated from ADCP. At the same time, we established a real time system of surface flow measurement by introducing a novel image collection system with high image compressibility. The performance of this system was confirmed by applying it to a small flood that occurred in the Sumiyoshi River.

INTRODUCTION

Measurement of velocity distribution in river flow especially in flood conditions is very important and, at the same time, it is very difficult-to-measure hydrological parameters. Probe type instruments such as a current meter or an electromagnetic velocity meter are difficult and dangerous to employ for a situation in which flood flow contains debris or driftwood. A primitive as well as traditional method applies floats. However, it is not easy to drop them in a transverse direction without a bridge. Even when a bridge or a float dropping system is available, operating the system poses difficulty in large flood because of extremely dangerous conditions due to the high water as well as waves. Moreover, traceability of floats to flow streams is questionable in an intensive turbulent conditions that accompanies large vortices. In recent years, a sophisticated instrument such as an acoustic Doppler current profiler (ADCP) (Muste, et al. (1), Dinehart and Burau (2) and Yorozuya et al. (3)), which can measure three dimensional velocity distributions below a transducer, has been available for river flow measurement. Recently, improvement of a tethered ADCP platform enables us to employ ADCP measurement even in torrential flow (Yorozuya et al. (4)). However it is not always possible to measure a peak discharge and at the same time it requires much labor to conduct continuous measurements during floods. On the other hand, H-ADCP is available for continuous measurements (Nihei and Kimizu (5)); though, it cannot be used for small scale or shallow rivers. Alternative methods are so-called non-intrusive methods such as UHF radar (Wang et al. (6)), radio current-meter (Yamaguchi and Niizato (7)) or imaging techniques (Fujita and Komura (8), Fujita et al. (9-11), Hauet et al. (12), and Muste et al. (13)). Common characteristic features of the non-intrusive methods is that they trace advection speeds of surface ripples generated by various causes such as open-channel turbulence, wind shear or hydraulic structures; therefore, such methods rely on the assumption that the advection speed represents the water surface flow velocity. This assumption has been verified indirectly so far by comparing discharge values calculated by compiling velocity distributions, velocity index and water depth. However, direct comparison with the other methods has been rarely conducted in the field conditions, except in the research conducted by Sun et al. (14). Therefore, we conducted simultaneous measurements by means of imaging techniques and an ADCP to examine the reliability of the assumption regarding the advection speed of surface ripples. In addition, we developed a real time measurement system for river surface flow by adopting a novel image collection system with high image compressibility and introducing it to the Sumiyoshi River which is a typical small scale river in Kobe City.

MEASUREMENT SITE

The observation site in the present study is a section downstream of the Heisei Ohashi Bridge near Maebashi City located more than 180km upstream from the river mouth of the Tone River in Japan. Since the observation site has a steep slope as well as larger bed materials, alternate bars were developed which produced variation in water surface widths in normal flow conditions as shown in Fig.1. The measurement line was selected at the narrower section with a large bar on its left as shown in Fig.1. Since the water surface slope is locally steep with a faster flow, water surface ripples were observed even in normal flow conditions. The width of the measurement section was about 30m. The maximum water depth during the measurement was about 2m and the estimated local Froude number was about 0.8.

Measurements of the three dimensional velocity distributions were conducted by using an acoustic Doppler type instrument, which is the Work Horse ADCP with 1200 kHz manufactured by Teledyne RDI instruments with commands shown in Table 1, a global positioning system, which is the VRS-RTK-GPS; DELTA manufactured by JAVAD whose horizontal-positioning accuracy is $10\text{mm} + 1.0\text{ppm} \times \text{base-length}$, and a tethered ADCP platform, which is a high speed river boat manufactured by Ocean Science. With compiling these devices, the authors traversed them with a wire-traverse

line along the section pulling by human power. As indicated in Fig.2, the traverse line of the boat is somewhat skewed due to the drag force acting upon it. The measurement data at each point is projected onto a transverse straight line based on the assumption that the velocity distribution does not change in a short longitudinal distance. Since ADCP cannot measure three dimensional velocity components near the water surface as well as near the river bed, the velocity at the water surface is extrapolated in a vertical direction using four different methods, such as (i) the constant method, (ii) the three points

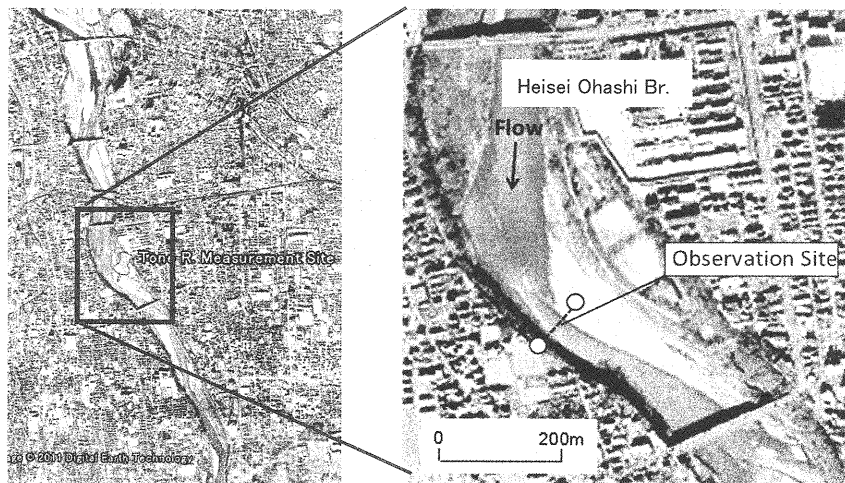


Fig.1 Location of the observation site in the Tone River in Maebashi City, downstream of the Heisei Ohashi Bridge; about 180km from the river mouth

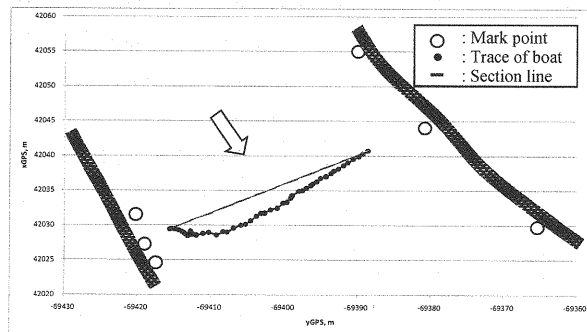


Fig.2 Measurement section and trace of boat-mounted ADCP

slope method, (iii) the power method as well as (iv) one applying a logarithmic profile. As Conzalez-Castro and Muste (15) introduced, the constant method assumes that velocities in un-measured-upper layer are identical to observed value at the nearest good-quality value from transducer, while the three points slope method assumed that the velocity at the un-measured-upper layer has a linear relation, whose line is determined using upper three points from the transducer. Regarding the power law, the velocity values in the un-measured-upper layer were estimated using the least square method assuming the power distribution employing whole observed values by ADCP. In addition, the logarithmic profile was also

implemented as Rennie et al. (16) as well as Sime et al. (17) employed for estimating shear velocities. Though the four different methods were introduced, no conclusive results have been established. Therefore, the authors of this paper obtained four different values, and calculated the average and the standard deviation assuming the averaged values indicates the true velocity estimated by ADCP. The six circles in Fig.2 indicate the mark point locations employed for establishing the mapping relation between the physical and the screen coordinates by assuming that the water surface is flat. The mark point coordinates are obtained by using a RTK-GPS which is mounted on the same boat in which the ADCP

Table. 1 Commands of ADCP

Mode of Bottom truck	BM5: normal
Pings for Bottom truck	BP3: 3pings
Pings for Water truck	WP3: 3pings
Type of band	WB0: Broad band
Disntave of first blank	WS10: 10cm
Mode of measurement	WM12: high speed mode
Number of layer	WN50: 50 layers
Thickness of layer	WS10: 10cm

instrument is installed and by keeping its position for about one minute. Such a procedure enables the mark points to be located in the water zone near each river bank as illustrated in Fig.2. Mark points can be placed on each bank if the relative height from the water surface is available.

SURFACE FLOW MEASUREMENT BY IMAGING TECHNIQUES AND ADCP

A typical image analysis technique for flow fields in laboratory scale experiments is the particle image velocimetry (PIV), in which two dimensional velocity distributions in a laser light sheet can be measured from consecutive image pairs. Fujita and Komura (8) and Muste et al. (13) extended the target of PIV to river surface flow measurements and termed it the large-scale PIV (LSPIV). As aforementioned, unseeded imaging techniques as well as a radar technique tracks the advection of surface ripples, i.e. irregularities in the light reflection from a water surface viewed from an oblique angle. Fig.3 shows surface ripple features utilized in the present measurement as well as locations of mark point on the water surface near the shorelines. The image was recorded using a high-density video camera attached on a tripod placed on the right bank as illustrated in Fig.4. The size of the captured image is 1920 by 1080 pixels and the angle of repose covering the water surface varies between 7.5 and 23 degrees, which are favorable values in view of oblique flow measurements in imaging techniques. Fig.3 shows that the water surface is forced to deform randomly due to turbulence generated at the gravel river bed, while generating whitecaps in the middle of the river where the velocity seems to be the highest. From the original video, it can be easily observed that the surface features are advected in a downstream direction at almost a constant speed. The issue in contention is whether such advection speed of surface feature represents the surface velocity for sure or something else. To examine this matter, we utilized two types of image analysis methods, i.e. LSPIV and STIV (10) and compared their results with those estimated by ADCP measurements.

In the application of LSPIV, the distorted images are corrected by using the previously-mentioned mapping relation between the physical and screen coordinates with additional information of water level under the same coordinate system. The pixel size used for the image transformation is 0.08m in the present case. The transformed image is shown in Fig.5. The number of images used in LSPIV is 500 frames sampled at a rate of 30 fps. The particle image velocimetry (PIV) is then applied to the transformed images with an interrogation window size of 40 by 40 pixels. Sixty interrogation windows

were allocated on a straight line with a spacing of 0.53m as shown in Fig.5(a) as a series of rectangles, which lie on the same section line as in the ADCP measurement. The physical size of the interrogation window is 3.2m by 3.2m and the

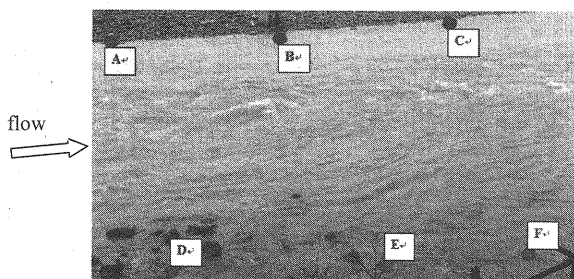


Fig.3 Surface ripples at the measurement section of the Tone River; circles are mark point locations.

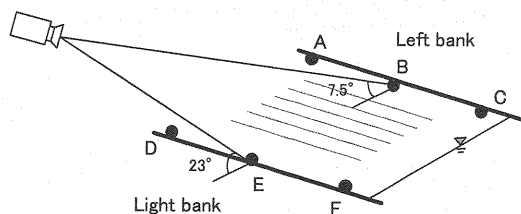


Fig.4 Angle of repose for image shooting

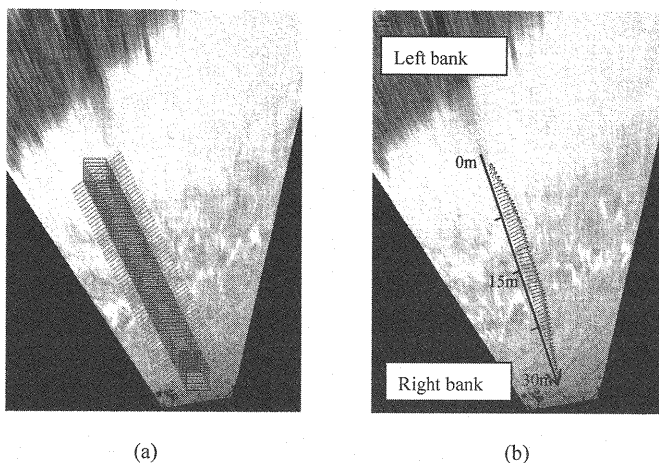


Fig.5 Application of LSPIV to surface images; left: the arrangement of interrogation window, right: analyzed velocity distribution

time separation between image pair is set as 0.0667 seconds. The analyzed result is illustrated in Fig.5(b), which provides evidence that the velocity increases gradually towards the center of the river and also decreases closer to the other side of the river bank. This phenomenon suggests that the surface features are advected not in a random manner but follow the surface velocity at least in a qualitative manner at this stage of the data processing.

In STIV, a time averaged velocity along an inspection line directed towards the streamwise direction can be obtained by applying the gradient tensor method to a space time image (STI) (10). The arrangement of inspection lines in the present analysis is shown in Fig.6. We chose sixty inspection lines, which is the same number of interrogation windows in LSPIV. The physical length of an inspection line was kept constant at 8.1 m assuming uniformity of flow along its line within this distance. The inspection lines were prepared so that their middle points pass through the section line for the



Fig.6 Arrangement of inspection lines in STIV

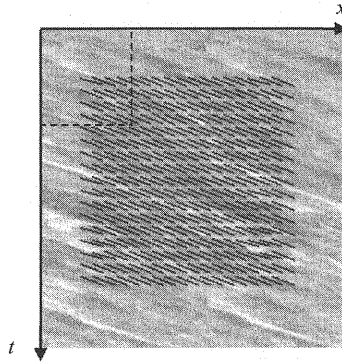


Fig.7 Space time image for an inspection line and gradient vectors obtained by STIV

other measurements. Since the images are taken from an oblique angle, the length of each STI varies gradually in the transverse direction. An example of STI is shown in Fig.7 together with the analyzed orientation angles by STIV. Here, we applied the image filtering method with a two-dimensional fast Fourier transformation to improve the quality of the STI through a band pass filter in a wave number domain, which we refer to as HL-STIV (11). For the purpose of efficiency, the size of the STI was modified so that its vertical and horizontal length becomes 256 by 256 pixels by repeatedly reusing a part of STI without making any distortion. This modification of STI does not influence the accuracy of STIV, because it tries to detect the average gradient of the orientation vector in the image and the information on image orientation is preserved in the present process of image reconstruction. The calculation of the orientation vector starts from an inspection window at the upper left corner as shown in Fig.7. The size of the inspection window was set at 40 by 40 pixels in the present case. By shifting the position of the inspection window step by step a total of 289 vectors were obtained as shown in Fig.7. The mean velocity for an inspection line can be calculated by averaging the angle of orientation vectors using coherency as a weighting function. The coherency is an index of clearness of image pattern which takes a value of zero for white noise and unity for a clear line.

As for the ADCP measurement, a cross-sectional velocity distribution obtained by ADCP at the measurement section is shown in Fig.8. The scattered data near the center of the channel indicates the difficulty in obtaining ADCP measurements with a boat in such severe flow conditions. Actually ADCP measures relative velocity, while GPS measures velocity of the boat. Thereafter, water velocities which should be measured by the system obtained by combining these two instruments. Although idealistic movement of the boat should be smooth for a better observation, actual behavior of the boat involves an abrupt movement especially in the middle of river only in such a difficult case. Unfortunately the movement makes boat speed high in streamwise direction; therefore, observed water velocity scatters to greater extent in

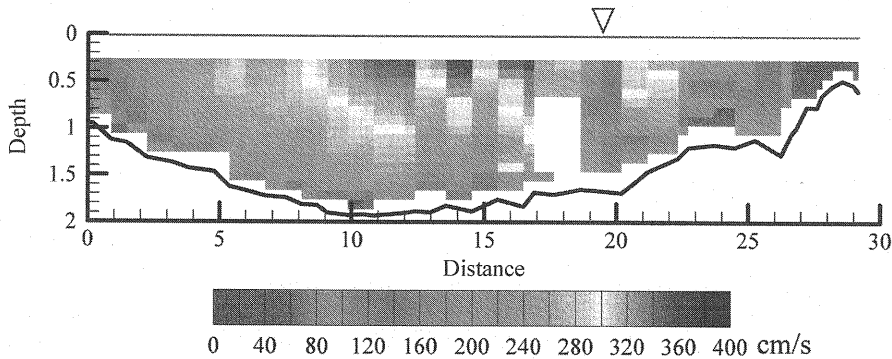


Fig.8 Streamwise velocity distribution at measurement section by ADCP

this area only. Difference of sampling time is another source of different values in the both measurements, i.e. thirty seconds or more in imaging methods, while less than few seconds in ADCP at the points of interest. As mentioned previously, the surface velocity distribution was extrapolated by applying the four different methods as well as averaging them at each single ensemble. Thereafter, the surface velocity distribution obtained by ADCP was compared with those measured by LSPIV and STIV as shown in Fig.9. With regarding to ADCP measurements, the averaged values as well as the standard deviation were also indicated as $ADCP_average$, and $ADCP_ave \pm std$, respectively. As can be easily understood from the previous discussion in terms of ADCP measurements, the surface velocity distribution displays a significant scatter especially between 13.0m and 24.0m from the left bank. On the other hand, the imaging techniques both yield smooth variation in their distributions, because they focus to a fixed point or a line for more than several tens of seconds and thus generate smoother variations through the elimination of unsteadiness as well as noise in the measurement. The important point is that even with some scatter in the respective data, measurements by the three methods yield almost equivalent velocity distributions in most of the region. This fact strongly supports the aforementioned assumption regarding the equivalence between a surface flow velocity and an advection speed of surface features. Regarding the imaging techniques, there appears some difference between LSPIV and STIV especially near the bank. This difference is due to the saturation of image intensity near the left bank by the sunlight reflection, which becomes the source of error in the measurement by STIV because image orientation in STI disappears in such a condition. As an additional discussion, three different methods in Fig.9, especially in the range between 0.0m and 13.0m, were redrawn in Fig.10 whose horizontal axis is the water surface velocity by ADCP while vertical axis is that by image techniques. As indicated, STIV has slightly higher values compared with ADCP while most of the vales by LSPIV are on the line of the 45 degree angle. As for the relation between ADCP and LSPIV a correlation coefficient; r^2 , is equal to 0.85. Surface velocity distributions thus obtained by imaging techniques can be used to estimate discharge at the measurement section by multiplying a

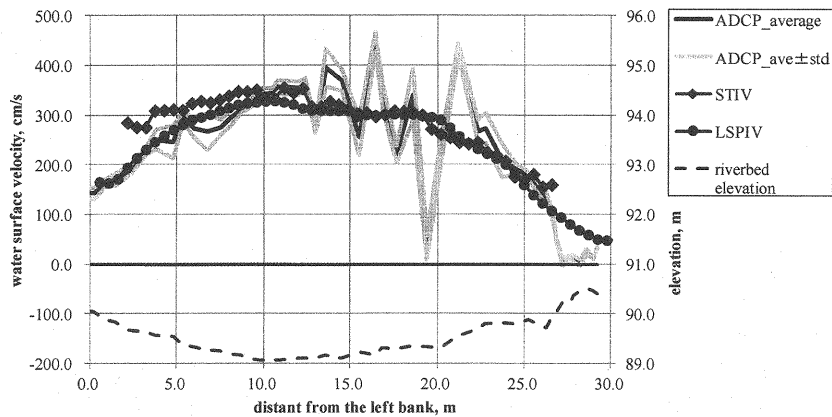


Fig.9 Surface velocity distributions obtained by various methods and bed elevation

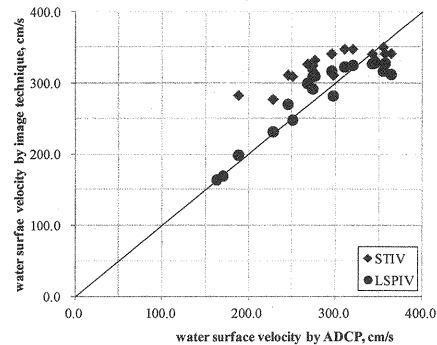


Fig.10 Surface velocity distributions obtained by various methods and bed elevation

conventional index value of 0.85 to the surface velocity and integrating it over the cross-sectional area. According to this procedure, STIV yielded a discharge of $100.5 \text{ m}^3/\text{s}$ while LSPIV result gave $98.6 \text{ m}^3/\text{s}$. On the other hand, ADCP that measures most of the cross-sectional velocity distribution except near the water surface yielded a discharge of $99.6 \text{ m}^3/\text{s}$, which is close to the results by imaging techniques. Considering scatter and deficiency of data by ADCP near the center of the river shown in Fig.8, the measurement data by means of STIV or LSPIV seems to yield a more reliable data in the present case.

EFFICIENT MANAGEMENT SYSTEM FOR RIVER MONITORING

A novel image management system

In developing a real-time river monitoring system, a crucial issue is how to store or transmit image data efficiently, since the size of image data; e.g., movie file, is significantly larger than that of a still image as well as it is difficult to store a long span of image data to a recording system. Therefore, a system with high image compressibility as well as a system manageable via the internet is required. One of the systems that meets the above requirement is the Super Guard XP treated

by AR BROWN Co. Ltd, whose system utilizes the high image compressibility technique termed SMICT based on the Motion-JPEG images with a size of 640 by 480 pixels and output a movie file at least every ten minutes. The file size changes dynamically from several megabytes to about 200 megabytes for a ten-minute movie file depending on the ratio of image area with or without motion. Usually, the file size is very small for a normal flow condition with little variation in surface features while it accumulates in considerable amounts for a flood flow condition with time-varying surface features. The minimum image sampling rate is 15 frames per second (fps) which allows the application of imaging techniques. When we use a one terabyte hard disk (HD), all of the image data for about a month can be stored on it by using an analogue camera installed near the river bank.

The advantage of this system is its capability to monitor the river through the internet. A ten-minute movie file successively stored on a HD of a PC locally installed at a measurement site can be transferred to a laboratory office via the internet, which can make us browse real-time images even at an office as well. Therefore, monitoring of multiple locations becomes possible if we install such a river monitoring system at an appropriate location accessible to the Internet. The important point is that the quality of a movie should not change at all even if the number of cameras are increased because the system itself is distributed independently. This aspect is quite different from a so-called web camera system conventionally used in river monitoring, in which image sampling rate varies significantly due to the restriction of data transfer capability, i.e. frame dropping occurs inconsistently; therefore, the application of imaging techniques poses difficulty if the image sampling rate reduces to a few frames per second. In this respect, it should be noted again that the new system is stable and is capable of capturing images at 15 fps which is favorable to use in imaging techniques.

Installation of the system to the Sumiyoshi River

In the present study, two cameras were installed in the Sumiyoshi River near Uosaki Station of the Rokko Liner railway in Kobe City supported by the local government. The cameras were attached to a pole on the left bank about three meters above the ground. A general view of the measurement location and a camera angle is provided in Fig.11. A control box contains a PC with analogue image capturing boards as well as a 1TB-HD. The channel width is about 20m at the section including side walkways. We implemented a wired internet connection in the present case because high-speed wireless connection was still unstable at the time of system installation. Analogue cameras capable of being used even at nighttime by infrared illumination were selected. The images from the two cameras captured during the daytime and at nighttime are shown in Fig.12. Camera 1 was prepared so that it covered a longer river reach for capturing a longitudinal water surface profile while camera 2 was set for surface flow measurements. Fig.12(c) and (d) were captured for the same small flood at daytime and nighttime respectively. The daytime images capture the generation of surface features with fairly good ripples, but the nighttime image contains random noise due to the reflection from raindrops by infrared illumination.

Application of STIV

In the present study, STIV was applied to a small flood generated by a localized torrential rain that continued from Jun 26 to 27 in 2010. The peak rain intensity was 16mm/hr according to the hyetograph of the Sumiyoshi River basin shown in Fig.13. The surface features indicated in Fig.12(c) and (d) show similarity to those of the Tone River previously presented in Fig.3. Therefore, as was verified in the Tone River, we can assume here that the advection speed of such surface features represent the surface flow as well. A rough estimate of the Froude number was about 0.7. In order to

establish a real time system, video images deteriorated by a raindrop effect are shown in Fig.12(d) have to be taken care for continuous measurements with fewer efforts. For this purpose, we utilized the FFT image filtering as was used in the Tone River measurements. Fig.14 shows two STIs for the search line indicated in Fig.12(d) before and after the application of the FFT filtering. Horizontal short noises caused by rain drops are eliminated clearly after the FFT filtering and STIV yields almost constant orientation vectors successfully. Therefore, we utilize such a procedure in the following analysis as well.

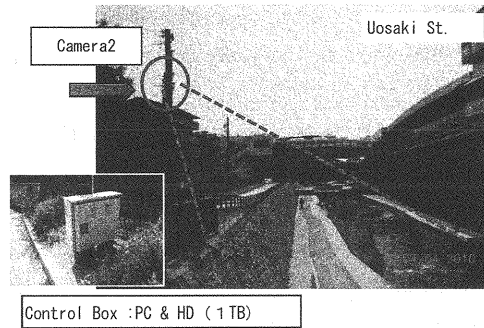


Fig.11 Location of monitoring camera 2

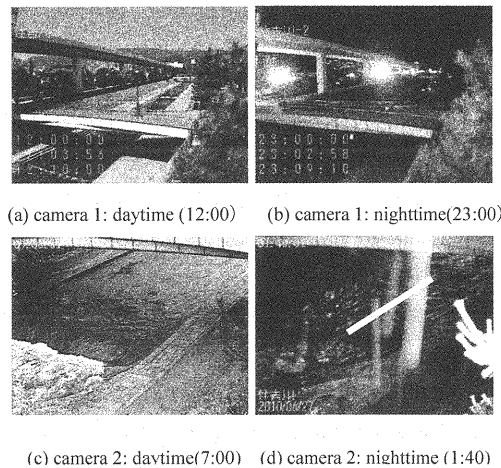


Fig.12 Field of view for the two cameras

Compared with the STIV, it should be noted that LSPIV is incapable of being used in such adverse conditions, such as the raindrop effect.

Fig.15 shows a transverse velocity distribution obtained by STIV when the lower channel reached a bankful stage at 1:40 am on July 27, which is the same flow as indicated in Fig.12(d). Surface velocity is almost uniform at 2.2m/s except for a region influenced by the vegetation zone upstream of the measurement section. The discharge at this stage was 9.6 m³/s. The stage discharge relation obtained by applying STIV at various stages is shown in Fig.16, with a favorable result allowing some scatter. The data scatter might have been caused by the error in stage information because its value was read from the water level from the image by utilizing physical height of several steps on the lower right bank as a reference scale. Fig.17 shows the relation between discharge and surface velocity at the channel center. It should be noted that the surface

velocity correlates with discharge better than the water depth since the cross-sectional shape is simple at the measurement location.

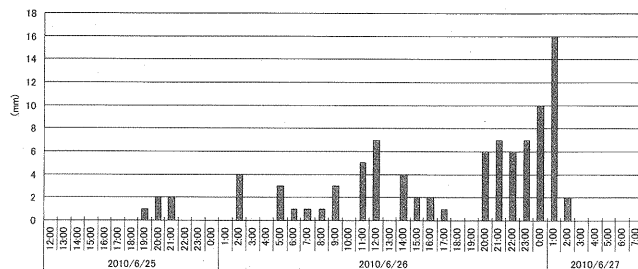


Fig.13 Hyetograph of the Sumiyoshi River

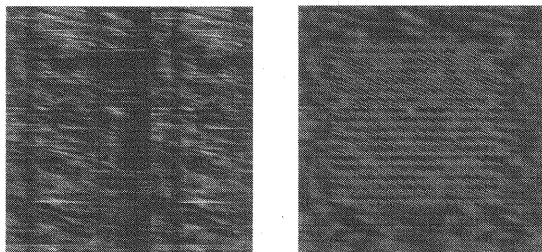


Fig.14 Effect of image improvement of STI under heavy rain for a search line in Fig.12(d); left original, right after FFT filtering

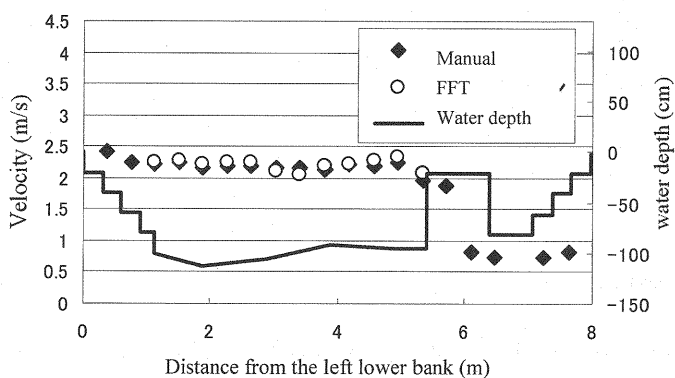


Fig.15 Surface velocity distribution measured at night: 1:40am June27, 2010

Realtime system for surface flow measurement

We developed a real time measurement system based on the STIV procedure incorporating with the image capturing system explained in previous sections. A flow chart of the system is provided in Fig.18. The system is composed of two independent systems: STIV and the image capture system (Super Guard XP). First, thirty seconds of a movie file captured by the system is discretized into a series of static JPG images of 450 frames in five minutes; then, the images are stored in a

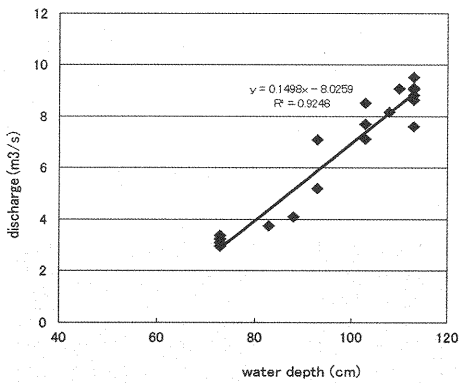


Fig.16 Rating curve of 2010 flood of the Sumiyoshi River

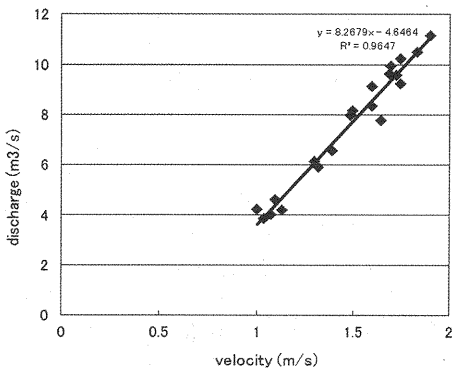


Fig.17 Discharge velocity relation of 2010 flood of the Sumiyoshi River

common folder. Secondly, the stored images are used in STIV for analyzing surface velocity distributions in about 90 seconds. Finally, the STIV system output the velocity information to a designated folder. The STIV process waits for ten minutes under a timer control until a new set of image files overwrite the previous files. The system which we developed was found to perform well without any problems for a day when we tentatively supplied the continuous image files of the Sumiyoshi River.

CONCLUSION

Measurements of a river surface velocity distribution by three different methods, i.e. ADCP, LSPIV and STIV were conducted in the upstream reach of the Tone River. Despite the difference in measurement techniques, the surface velocity

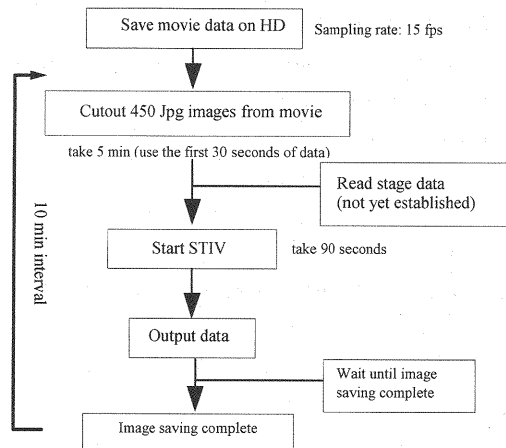


Fig.18 Flow chart of real time measurement system

distribution extrapolated from ADCP data agreed well with those obtained by imaging techniques, demonstrating the validity of the assumption that the water surface ripples are advected with the surface velocity. This finding provides evidence of the applicability and reliability of the imaging techniques as a non-intrusive river flow measurement method. Among the imaging techniques, STIV using FFT filtering to STI was found to be more robust than LSPIV through its application to the Sumiyoshi River Flood under a heavy rain. The influence of raindrops on STI was clearly eliminated by applying 2D-FFT image filtering. In measuring the Sumiyoshi River flood, monitoring cameras were installed at the river bank and consecutive images were captured successfully by a novel image capturing system based on Internet connections. The system is capable of capturing images at 15fps, which is much more reliable and stable than the conventional web camera system. Furthermore, a real time system based on this image capturing and STIV systems were developed, which is capable of analyzing a surface velocity distribution and a discharge at a sampling rate of ten minutes. The system developed in this study is both robust and stable even under heavy rain conditions. The system needs to be improved so that stage data from water level gage can be directly incorporated into the STIV analysis. Further application of the system to a larger scale river is necessary to demonstrate its reliability and effectiveness.

ACKNOWLEDEMENTS

We are grateful to the financial support by the Kinki Kensetsu Association in the latter part of this research. We are also grateful to the supports by the local government of Hyogo Prefecture and the Osaka Sokki Jigyo co. Ltd. in installing monitoring cameras at the Sumiyoshi River.

REFERENCES

1. Muste, M., Fujita, I., and Hauet, A.: Large-scale particle image velocimetry for measurements in riverine environments, *Water Resources Research*, Vol.44, W00D19, doi:10.1029/2008WR006950, 2008.
2. Dinehart, R. L. and Burau, J. R.: Averaged indicators of secondary flow in repeated acoustic Doppler current profiler crossings of bends, *Water Resources Research*, Vol.41, W09405, pp.1-18, 2005.
3. Yorozuya, A., Kanno, Y., Fukami, K. and Oodaira, K. : Development of automatic water discharge measurement system, *Environmental Hydraulics -Christodoulou & Stamou (eds)*, pp. 839-844, 2010.
4. Yorozuya, A., Okada, S., Kistuda, T., Kanno, Y., and Fukami, K. : Proposal of tethered ADCP platform for high-speed flow measurements, *Advances in River Engineering*, Vol.16, pp.59-64, 2010.
5. Nihei, Y. and Kimuzi, A.: A new monitoring system for river discharge with an H-ADCP measurement and river-flow simulation, *JSCE Journal of Hydraulic, Coastal and Environmental Engineering*, Vol.63, No.4, pp.295-310, 2007 (in Japanese).
6. Wang, C.J., Wen, B.Y., Ma, Z.G., Yan, W.D. and Huang, X.J.: Measurement of river surface currents with UHF FMCW radar systems, *Journal of electromagnetic waves and applications*, Vol.21(3), pp. 375-386, 2007.
7. Yamaguchi, T. and Niizato, K.: Flood discharge observation using radio current meter, *JSCE Journal of Hydraulic, Coastal and Environmental Engineering*, Vol.497/II-28, pp.41-50, 1994 (in Japanese).
8. Fujita, I. and Komura, S.: Application of video image analysis for measurements of river-surface flows, *Annual Journal of Hydraulic Engineering*, Japan Society of Civil Engineers, Vol.38, pp.733-738, 1994 (in Japanese).
9. Fujita, I., Muste, M. and Kruger, A.: Large-scale particle image velocimetry for flow analysis in hydraulic engineering applications, *Journal of Hydraulic Research*, Vol.36, No.3, pp.397-414, 1998.
10. Fujita, I., Watanabe, H. and Tsubaki, R.: Development of a non-intrusive and efficient flow monitoring technique: The space time image velocimetry (STIV), *International Journal of River Basin Management*, Vol.5, No.2, pp.105-114, 2007.
11. Fujita, I., Ando, T., Tsutsumi, S. and Hara, H.: Efficient space-time image analysis of river surface pattern using two dimensional fast Fourier transformation, *Proceedings of 33rd IAHR Congress*, pp.2272-2279, 2009.
12. Hauet, A., Creutin, J.-D. and Belleudy, P.: Sensitivity study of large-scale particle image velocimetry measurement of river discharge using numerical simulations, *Journal of Hydrology*, Vol.349(1-2), pp.178-190, doi:10.1016/j.jhydrol.2007.10.062, 2008.
13. Muste, M., Yu, K. and Spasojevic, M.: Practical aspects of ADCP data use for quantification of mean river flow characteristics; part I: Moving-vessel measurements, *Flow Measurement and Instrumentation*, Vol.15, No.1, pp.1-16, 2004.
14. Sun, X., Shiono, K., Chandler, J. H., Rameshwaran, P., Sellin, R.H.J. and Fujita, I.: Discharge estimation in small irregular river using LSPIV, *Water Management*, Vol.163 Issue WM5, pp.247-254, 2010.
15. Conzalez-Castro, J. and Muste, M.: Framework for estimating uncertainty of ADCP measurements from a moving boat by standardized uncertainty analysis, *Journal of Hydraulic Engineering*, Vol.133, pp.1390-1410, doi:10.1061/(ASCE)0733-9429(2007)133:12(1390)
16. Rennie, C.D., et al.: Measurement of bed load velocity using an Acoustic Doppler Current Profiler, *Journal of Hydraulic Engineering*, Vol. 128, pp. 473-483, doi:10.1061/(ASCE)0733-9429(2002)128:5(473)
17. Sime, L. C., et al.; Estimating shear stress from moving boat acoustic Doppler velocity measurements in a large gravel bed river, *Water Resources Research*, Vol. 43, W03418, doi:10.1029/2006WR005069, 2007.

(Received Jul, 21, 2011 ; revised Feb, 17, 2012)